

FLIC Fermions and Hadron Phenomenology

D. B. Leinweber^{1 a}, J. N. Hedditch¹, W. Melnitchouk^{1,2}, A. W. Thomas¹, A. G. Williams¹, R. D. Young¹,
J. M. Zanotti¹, and J. B. Zhang¹

¹ Centre for the Subatomic Structure of Matter and Department of Physics and Mathematical Physics, University of Adelaide, Adelaide, SA 5005, Australia

² Jefferson Lab, 12000 Jefferson Avenue, Newport News, VA 23606, U.S.A.

Received: 27 September 2002

Abstract. A pedagogical overview of the formulation of the Fat Link Irrelevant Clover (FLIC) fermion action and its associated phenomenology is described. The scaling analysis indicates FLIC fermions provide a new form of nonperturbative $\mathcal{O}(a)$ improvement where near-continuum results are obtained at finite lattice spacing. Spin-1/2 and spin-3/2, even and odd parity baryon resonances are investigated in quenched QCD, where the nature of the Roper resonance and $\Lambda^*(1405)$ are of particular interest. FLIC fermions allow efficient access to the light quark-mass regime, where evidence of chiral nonanalytic behavior in the Δ mass is observed.

PACS. 12.38.Gc Lattice QCD calculations – 12.38.Aw General properties of QCD (dynamics, confinement)

1 FLIC Fermions

The CSSM lattice collaboration has been examining the merits of a new lattice fermion action [1] in which the (irrelevant) operators introduced to remove fermion doublers and lattice spacing artifacts are constructed with smoothed links. These links are created via APE smearing [2]; a process that averages a link with its nearest transverse neighbors in a gauge invariant manner. Iteration of the averaging process generates a “fat” link. The use of links in which short-distance fluctuations have been removed simplifies the determination of the coefficients of the improvement terms [3]. Perturbative renormalizations are small for smeared links and tree-level estimates, or the mean-field improved estimates used here, are sufficient to remove $\mathcal{O}(a)$ errors in the lattice spacing a , to all orders in the strong coupling g . The key is that both the energy dimension-five Wilson term and the Clover term [4] are constructed with smooth links, while the relevant operators, surviving in the continuum limit, are constructed with the original untouched links generated via standard Monte Carlo techniques. We call this action the Fat-Link-Irrelevant-Clover (FLIC) fermion action.

The established approach to nonperturbative (NP) improvement [5] tunes the coefficient of the clover operator to all powers in g^2 . Unfortunately, this formulation of the clover action is susceptible to the problem of exceptional configurations as the quark mass becomes small. Chiral symmetry breaking in the clover fermion action introduces an additive mass renormalization into the Dirac operator

that can give rise to singularities in quark propagators at small quark masses. In practice, this prevents the simulation of small quark masses and the use of coarse lattices ($\beta < 5.7 \sim a > 0.18$ fm) [3, 6].

The clover term of the fermion action requires a lattice determination of the QCD field strength tensor $F_{\mu\nu}$. The so-called clover version of $F_{\mu\nu}(x)$ involves the product of links around the four plaquettes centered at x in the μ - ν plane. This simple formulation is commonly used in clover actions, but it is now known to have large $\mathcal{O}(a^2)$ errors. These errors lead to 10% errors in the topological charge even on very smooth configurations [7].

A key feature of FLIC fermions is that the construction of irrelevant operators using smoothed links facilitates the use of highly improved definitions of the QCD field strength tensor $F_{\mu\nu}$. In particular, we employ an $\mathcal{O}(a^4)$ improved definition of $F_{\mu\nu}$ [8] in which the standard clover-sum of four 1×1 Wilson loops is combined with 1×2 , 1×3 , 2×2 and 3×3 Wilson-loop clovers.

The scaling analysis of FLIC fermions is performed at three different lattice spacings and two different volumes. The tree-level $\mathcal{O}(a^2)$ -Symanzik-improved [9] gauge action is used on $12^3 \times 24$ and $16^3 \times 32$ lattices with lattice spacings of 0.093, 0.122 and 0.165 fm determined from a string tension analysis incorporating the lattice Coulomb term [10]. Where necessary, we take $\sqrt{\sigma} = 440$ MeV. A total of 200 configurations are used in the scaling analysis at each lattice spacing and volume. In addition, for the light quark simulations, 94 configurations are used on a $20^3 \times 40$ lattice with $a = 0.134$ fm. The error analysis is performed by a third-order, single-elimination jackknife, with the χ^2 per degree of freedom obtained via covariance matrix fits.

^a Plenary talk presented by Derek Leinweber.

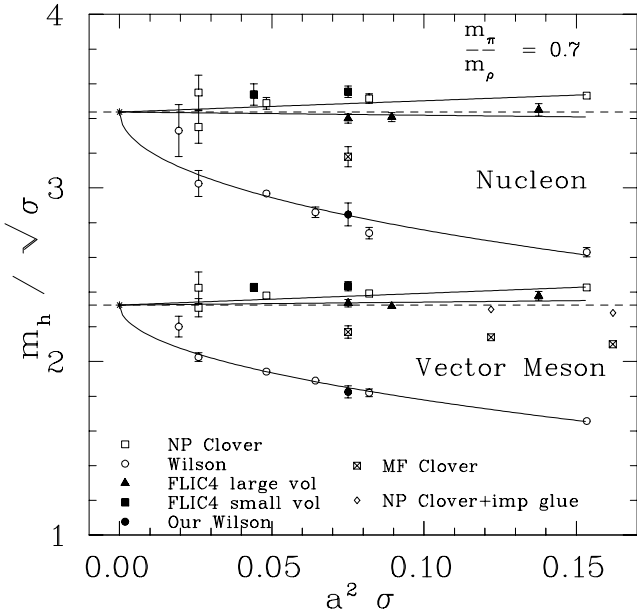


Fig. 1. Nucleon and vector meson masses for the Wilson, Mean-Field (MF) improved, NP-improved clover and FLIC actions obtained by interpolating simulation results to $m_\pi/m_\rho = 0.7$. For the FLIC action (“FLIC4”), fat links are constructed with $n = 4$ APE-smearing sweeps with smearing fraction $\alpha = 0.7$. Results from the CSSM lattice collaboration are indicated by the solid symbols; those from earlier simulations by open or hatched symbols. The solid-lines illustrate fits, constrained to have a common continuum limit, to FLIC, NP-improved clover and Wilson fermion action results obtained on physically large lattice volumes.

A fixed boundary condition and smeared sources [11] are used for the fermions.

Figure 1 displays our most comprehensive scaling analysis to date. The present results for the Wilson action agree with those of Ref. [12]. The FLIC action performs systematically better than the mean-field improved clover action and competes well with those obtained with the NP-improved clover fermion action [12].

Our two different volumes used at $a^2\sigma \sim 0.075$ indicate a finite volume effect, which increases the mass for the smaller volumes at $a^2\sigma \sim 0.075$ and ~ 0.045 . Examination of points from the small and large volumes separately indicates continued scaling toward the continuum limit. While the finite volume effect will produce a different continuum limit value, the slope of the points from the smaller and larger volumes agree.

Focusing on simulation results from physical volumes with extents ~ 2 fm and larger, we perform a simultaneous fit of the FLIC, NP-improved clover and Wilson fermion action results. The fits are constrained to have a common continuum limit and assume errors are $\mathcal{O}(a^2)$ for FLIC and NP-improved clover actions and $\mathcal{O}(a)$ for the Wilson action. An acceptable χ^2 per degree of freedom is obtained for both the nucleon and ρ -meson fits. These results indicate that FLIC fermions provide a new form of nonperturbative $\mathcal{O}(a)$ improvement. The FLIC fermion

results display nearly perfect scaling indicating $\mathcal{O}(a^2)$ errors are small for this action.

2 Baryon Resonances

Lattice studies of baryon excitations [13, 14, 15, 16, 17] provide valuable insight into the forces of confinement and the nature of QCD in the nonperturbative regime. They complement the high precision measurements of the N^* spectrum under way at Jefferson Lab. The simulations presented here are performed on 392 $\mathcal{O}(a^2)$ -Symanzik-improved [9] configurations of size $16^3 \times 32$ at $\beta = 4.60$ providing a lattice spacing of $a = 0.122(2)$ fm. FLIC fermions are implemented with 4 sweeps of APE smearing at $\alpha = 0.7$.

2.1 Spin-1/2 Baryon Resonances

There are two nucleon interpolating fields commonly considered in exciting the nucleon from the vacuum. The standard interpolating field couples a u - d quark pair to a scalar diquark and is $\mathcal{O}(1)$ in a nonrelativistic reduction. The alternate interpolator is $\mathcal{O}(p^2/E^2)$ in a nonrelativistic reduction placing two quarks in relative P waves. Odd-parity states may be projected from correlation functions of these interpolators. The standard interpolator is expected to have stronger overlap with the lowest-lying odd-parity state due to the scalar-diquark construction of the interpolator.

In Fig. 2 we show the N and $N^*(1/2^-)$ masses from FLIC fermions as a function of m_π^2 . For comparison, we also show results from simulations with Wilson [17] and domain wall fermions (DWF) [16], and the NP-improved clover action [15] with different source smearing and volumes. There is excellent agreement between the different improved actions for the nucleon mass. The Wilson results lie systematically low in comparison to these due to large $\mathcal{O}(a)$ errors in this action [1].

A similar pattern is seen for the lowest-lying $N^*(1/2^-)$ masses. A mass splitting of approximately 400 MeV is clearly visible between the N and N^* for all actions, including the Wilson. The trend of the $N^*(1/2^-)$ data with decreasing m_π is also consistent with the mass of the lowest physical negative parity N^* state.

The mass of the $J^P = 1/2^+$ state obtained from the alternate nucleon interpolating field [13], which vanishes in a nonrelativistic reduction, is shown in Fig. 3. In addition to the FLIC and Wilson results from the present analysis, also shown are the DWF results [16], and results from an earlier analysis with Wilson fermions analyzed via the operator product expansion [13]. The most striking feature of the data is the relatively large excitation energy of the N' , some 1 GeV above the nucleon. It has been speculated that the alternate interpolator may have overlap with the lowest $1/2^+$ excited state [16]. However, there is little evidence that this state is the $N^*(1440)$. It is likely that the alternate nucleon interpolator simply does not have good

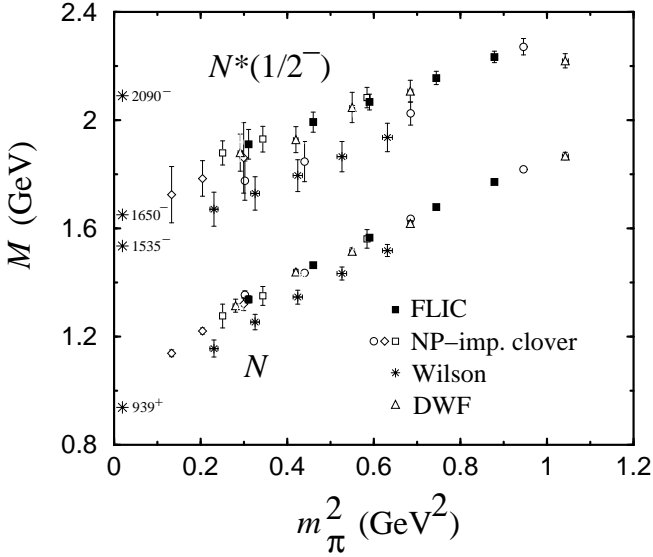


Fig. 2. Masses of the nucleon (N) and the lowest $J^P = 1/2^-$ excitation (“ N^* ”), obtained from the standard nucleon interpolating field. The FLIC and Wilson results are from the present analysis.

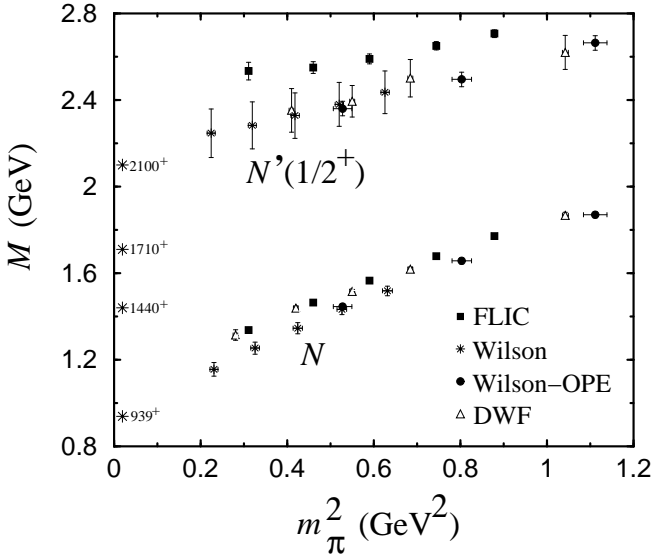


Fig. 3. Masses of the nucleon, and the lowest $J^P = 1/2^+$ excitation (“ N' ”) obtained from the alternate interpolating field. The FLIC and Wilson results are from this analysis.

overlap with either the nucleon or the Roper, but rather a (combination of) excited $1/2^+$ state(s).

The spectrum of positive and negative parity Λ states is shown in Fig. 4. Here we consider an interpolating field which contains terms common to the $SU(3)$ -flavor singlet and octet interpolating fields. It is the $SU(2)$ -isospin analogue of the Σ^0 interpolating field and does not bias the flavor symmetry of the Λ resonances. The positive (negative) parity states labeled Λ_1 (Λ_1^*) and Λ_2 (Λ_2^*) are constructed from the traditional and alternate Λ interpolators analogous to those of the nucleon. The pattern of mass splittings is similar to that observed for the N^* 's in Figs. 2

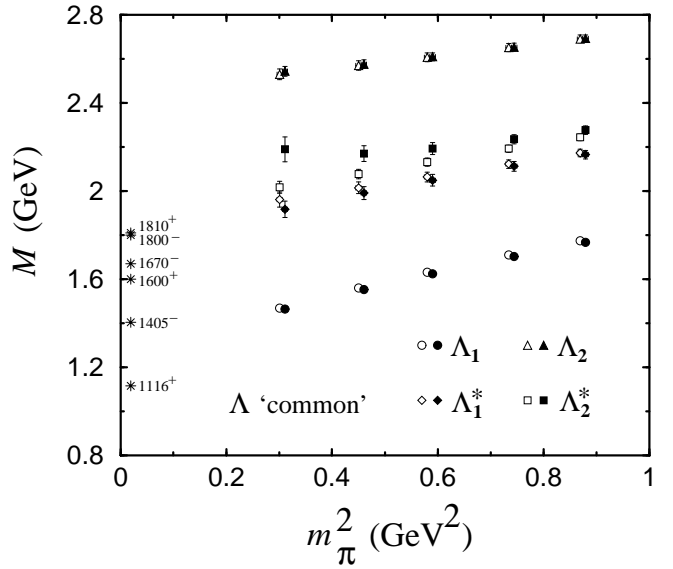


Fig. 4. Masses of the $\Lambda(1/2^\pm)$ states, obtained from the standard (Λ_1) and alternate (Λ_2) interpolating fields. The symbols are described in the text.

and 3. The importance of the correlation matrix analysis projecting the eigenstates of the Hamiltonian (filled symbols) is evident from a comparison with the naive fits to single correlation functions (open symbols). There is little evidence that the Λ_2 has any significant overlap with the first positive parity excited state, $\Lambda^*(1600)$ (c.f. the Roper resonance, $N^*(1440)$, in Fig. 3).

While it seems plausible that nonanalyticities in a chiral extrapolation [18] of N_1 and N_1^* results could eventually lead to agreement with experiment, the situation for the $\Lambda^*(1405)$ is not as compelling. Whereas a 150 MeV pion-induced self energy is required for the N_1 , N_1^* and Λ_1 states, 400 MeV is required to approach the empirical mass of the $\Lambda^*(1405)$. This large discrepancy suggests that relevant physics may be absent from simulations in the quenched approximation or perhaps more exotic interpolating fields are required to obtain significant overlap with the $\Lambda^*(1405)$. Investigations at lighter quark masses involving quenched chiral perturbation theory will assist in resolving these issues.

2.2 Spin-3/2 Baryon Resonances

We consider the following isospin-1/2, spin-3/2 interpolator [19]: $\chi_\mu^{N^+}(x) = \epsilon^{abc} (u^{T^a}(x) C \gamma_5 \gamma_\mu d^b(x)) \gamma_5 u^c(x)$, which transforms as a pseudo-vector under parity, in accord with a positive parity Rarita-Schwinger spinor. For the Δ^{++} resonance we use the standard interpolator as in Ref. [20]. Since the spin-3/2 Rarita-Schwinger spinor-vector is a tensor product of a spin-1 vector and a spinor, the spin-3/2 interpolating field contains spin-1/2 contributions. To project a spin-3/2 state one needs to use a spin-3/2 projection operator [21]. Following spin projection, the correlation function for a given spin still contains positive and negative parity states. In an analogous pro-

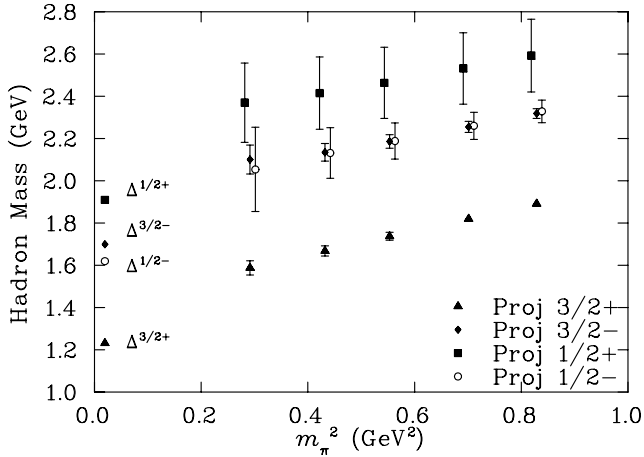


Fig. 5. Masses of the spin-parity-projected $\Delta(3/2^\pm)$ and $\Delta(1/2^\pm)$ states. The empirical masses are indicated along the ordinate.

cedure to that used for spin-1/2 resonances with a fixed boundary condition in the time direction, positive and negative parity states are obtained by taking the trace of the correlation function with the parity-projection operators $\Gamma_\pm = (1 \pm \gamma_4)/2$.

In Fig. 5 the spin-parity-projected $\Delta(3/2^+)$ (triangles) and $\Delta(3/2^-)$ (diamonds) masses are shown. We find a clear signal for the P -wave $\Delta(3/2^-)$ parity partner of the Δ ground state. The mass of the $\Delta(3/2^-)$ lies some 500 MeV above that of its parity partner. A discernible signal is detected for the $\Delta(1/2^\pm)$ states. The level ordering of the Δ states is consistent with that observed in the empirical mass spectrum.

In the isospin-1/2 sector, large statistical fluctuations make it difficult to obtain a clear signal, even with 392 configurations. Parity projecting to extract the $N(3/2^+)$ state, we find that the correlation function changes sign and has a large negative contribution for time slices in the range $t = 7-11$ following the source at $t = 3$. This behavior is an artifact associated with the quenched decay of the excited state into $N + \eta'$ and is further explored in Ref. [19].

The $N(1/2^+)$ channel also displays the interplay of a quenched decay channel and the ground state contribution. A strong P -wave coupling of the $N^*(1/2^+)$ to $N\eta'$ forces the correlation function to be negative at small times, which then turns positive at larger times when the ground state nucleon begins to dominate the correlation function. This suggests that the first excited state of the nucleon has a strong coupling to the quenched η' which remains degenerate with the pion in the quenched approximation. These results imply a gluon-rich structure for the Roper resonance and further indicate that it may be impossible to directly observe the Roper resonance at light quark masses in the quenched approximation. While there are claims to have observed the Roper in quenched QCD [22], these results follow from a Bayesian analysis, and the credibility of the Bayesian-prior information used in the analysis requires further examination [23,24].

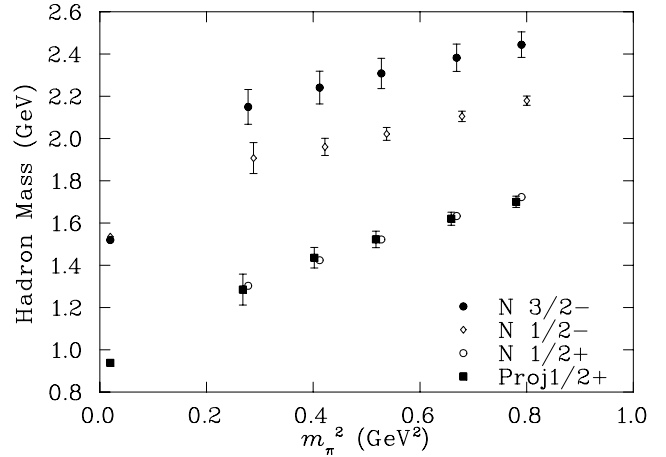


Fig. 6. Masses of the spin-projected $N(3/2^-)$ and $N(1/2^+)$ states, compared with the nucleon and $N(1/2^-)$ masses from Sec. 2.1.

The extracted masses of the $N(3/2^-)$ and $N(1/2^+)$ states are displayed in Fig. 6. Earlier results from Sec. 2.1 using the standard spin-1/2 interpolating field are also shown in Fig. 6 for reference. There is excellent agreement between the spin-projected $1/2^+$ state obtained from the spin-3/2 interpolating field and the earlier $1/2^+$ results.

3 Chiral Nonanalytic Behavior

The FLIC fermion action has extremely impressive convergence rates for matrix inversion [1,25], and this provides great promise for performing cost-effective simulations at quark masses closer to the physical values. Problems with exceptional configurations have prevented such simulations with Wilson-type fermion actions in the past.

In the absence of exceptional configurations, the standard deviation of an observable will be independent of the number of configurations considered in the average. Exceptional configurations reveal themselves by introducing a significant jump in the standard deviation as the configuration is introduced into the average. In severe cases, exceptional configurations can lead to divergences in correlation functions or prevent the matrix inversion process from converging.

The ease with which one can invert the fermion matrix using FLIC fermions leads us to attempt simulations down to small quark masses corresponding to $m_\pi/m_\rho = 0.35$. The simulations are on a $20^3 \times 40$ lattice with a physical length of 2.7 fm. We have used an initial set of 100 configurations, using $n = 6$ sweeps of APE-smearing and a five-loop improved lattice field-strength tensor. Preliminary results indicate exceptional configurations at the few percent level [19]. For the current results, these configurations have been identified and removed from the ensemble.

Figure 7 shows the N and Δ masses as a function of m_π^2 for eight quark masses. An upward curvature in the Δ mass for decreasing quark mass is observed in the FLIC fermion results. This behavior, increasing the quenched

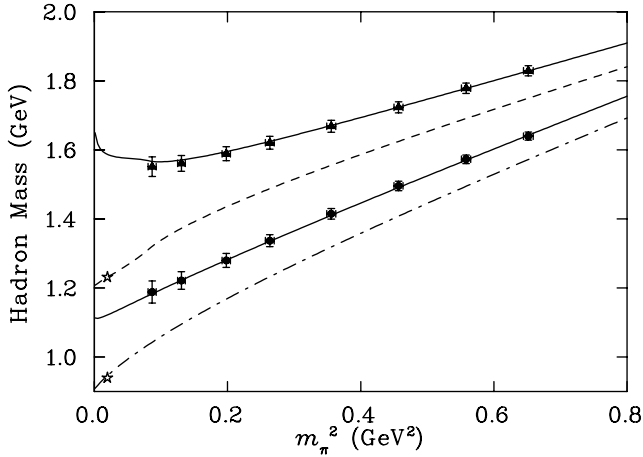


Fig. 7. Nucleon and Δ masses for the FLIC-fermion action on a $20^3 \times 40$ lattice with $a = 0.134$ fm. The solid curves illustrate fits of finite-range regulated quenched chiral perturbation theory to the lattice QCD results. The dot-dashed and dashed curves estimate the correction that will arise in unquenching the lattice QCD simulations for the N and Δ respectively. Stars at the physical pion mass denote experimental values.

$N - \Delta$ mass spitting, was predicted by Young *et al.* [26] using quenched chiral perturbation theory ($Q\chi PT$) formulated with a finite-range regulator. This $Q\chi PT$ fit to the FLIC-fermion results is illustrated by the solid curves. The dashed curves estimate the correction that will arise in unquenching the lattice QCD simulations. A similar preliminary analysis incorporating the light-meson cloud of the baryon octet is illustrated in Fig. 8. Inclusion of the kaon-cloud is in progress.

4 Conclusions

In constructing the irrelevant operators of clover fermion actions with APE-smearred links, FLIC fermions provide a new form of nonperturbative $\mathcal{O}(a)$ improvement. The technique allows the use of highly improved operators, provides optimal scaling and reduces the exceptional configuration problem. Quenched simulations at quark masses down to $m_\pi/m_\rho = 0.35$ have been successfully performed on a $20^3 \times 40$ lattice with a lattice spacing of 0.134 fm. Simulations at such light quark masses have already revealed the non-analytic behavior of quenched chiral perturbation theory in the Δ -baryon mass. We expect to see more evidence of chiral nonanalytic behavior in forthcoming simulations of the electromagnetic form factors of hadrons.

We thank the Australian National Computing Facility for Lattice Gauge Theory, and the Australian Partnership for Advanced Computing (APAC) for supercomputer time. This work was supported by the Australian Research Council. W.M. was supported by the U.S. Department of Energy contract DE-AC05-84ER40150, under which the Southeastern Universities Research Association (SURA) operates the Thomas Jefferson National Accelerator Facility (Jefferson Lab).

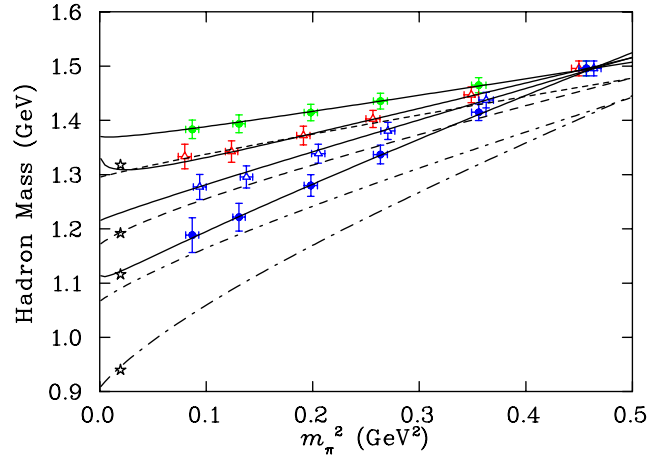


Fig. 8. Octet baryon masses for the FLIC-fermion action. Points are off set for clarity. Symbols are as described for Fig. 7.

References

1. J.M. Zanotti *et al.*, Phys. Rev. D **60**, 074507 (2002); Nucl. Phys. Proc. Suppl. **109**, 101 (2002).
2. M. Falcioni *et al.*, Nucl. Phys. **B251**, 624 (1985).
3. T. DeGrand (MILC collaboration), Phys. Rev. D **60**, 094501 (1999).
4. B. Sheikholeslami and R. Wohlert, Nucl. Phys. **B259** 572, (1985).
5. M. Luscher *et al.*, Nucl. Phys. **B478**, 365 (1996). M. Luscher *et al.*, Nucl. Phys. **B491**, 323, 344 (1997).
6. W. Bardeen *et al.*, Phys. Rev. D **57**, 1633 (1998); W. Bardeen *et al.*, Phys. Rev. D **57**, 3890 (1998).
7. F.D. Bonnet *et al.*, Phys. Rev. D **62**, 094509 (2000).
8. S. Bilson-Thompson *et al.*, Nucl. Phys. Proc. Suppl. **109**, 116 (2002); hep-lat/0203008.
9. K. Symanzik, Nucl. Phys. **B226**, 187 (1983).
10. R. G. Edwards *et al.*, Nucl. Phys. B **517**, 377 (1998) [hep-lat/9711003].
11. S. Gusken, Nucl. Phys. Proc. Suppl. **17**, 361 (1990).
12. R.G. Edwards, U.M. Heller and T.R. Klassen, Phys. Rev. Lett. **80**, 3448 (1998); see also R.D. Kenway, Nucl. Phys. Proc. Suppl. **73**, 16 (1999), for a review.
13. D. B. Leinweber, Phys. Rev. D **51**, 6383 (1995).
14. F. X. Lee and D. B. Leinweber, Nucl. Phys. Proc. Suppl. **73**, 258 (1999).
15. C. R. Allton *et al.*, Phys. Rev. D **47**, 5128 (1993); D. G. Richards *et al.*, Nucl. Phys. Proc. Suppl. **109**, 89 (2002); M. Göckeler *et al.*, Phys. Lett. B **532**, 63 (2002).
16. S. Sasaki, T. Blum and S. Ohta, Phys. Rev. D **65**, 074503 (2002).
17. W. Melnitchouk *et al.*, hep-lat/0202022; Nucl. Phys. Proc. Suppl. **109**, 96 (2002).
18. D. B. Leinweber *et al.*, Phys. Rev. D **61**, 074502 (2000).
19. J. M. Zanotti *et al.*, in preparation.
20. Y. Chung *et al.*, Nucl. Phys. **B197**, 55 (1982).
21. M. Benmerrouche *et al.*, Phys. Rev. C **39**, 2339 (1989).
22. F. X. Lee, *et al.*, Lattice '02, hep-lat/0208070; S. J. Dong, *et al.*, Lattice '02, hep-lat/0208055.
23. D. B. Leinweber, Phys. Rev. D **51** (1995) 6369.
24. C. Allton *et al.*, in preparation.
25. W. Kamleh *et al.*, Phys. Rev. D **66**, 014501 (2002).
26. R.D. Young *et al.*, hep-lat/0205017.